24th COBEM - 2017

24th ABCM International Congress of Mechanical Engineering
December 3-8, 2017, Curitiba, PR, Brazil

COBEM-2017-0766
NUMERICAL AND EXPERIMENTAL STUDY OF PRESSURE LOSS AT THE INTAKE MANIFOLD OF A FORMULA-SAE VEHICLE

Emerson da Trindade Marcelino
Álvaro Barbosa da Rocha
Luan Antonio Pereira Duarte Correia
Raimundo Nonato Calazans Duarte
Universidade Federal de Campina Grande, Department of Mechanical Engineering, R. Aprígio Veloso, 882 – CEP 58429140, Campina Grande, PB, Brazil
emerson.t.m.eng@gmail.com, alvarobarbosa2@hotmail.com, luan3p@gmail.com, raimundo.duarte@ufcg.edu.br.

Abstract. *The useful power developed by the naturally aspirated engine is a function of the mass of air drawn in due to a pressure gradient generated between the atmosphere and the combustion chamber. The International SAE Regulation makes requirements for flow reducers to be installed in the intake system of Formula-SAE vehicles, reducing the mass of air supplied to the combustion chamber and affecting the behavior of the engine as a whole due to the increased pressure drop. The objective of this paper was to numerically and experimentally analyze the pressure loss generated by the restrictor, measuring the impact on the volumetric efficiency and fuel consumption. The numerical analysis was performed in a CFD environment. The results have concluded the need to resize the intake system in order for the racing vehicle to be built meet the project's goal, which is to reach 100 kmph in less than 6 seconds, with a final speed of about 140 kmph.*

Keywords: *Experimental analysis, Formula-SAE, Engine, Intake system, CFD analysis.*

1. INTRODUCTION

In aspirated engines the air intake occurs because of the formation of a pressure gradient during the intake stroke. As the engine speed increases, the pressure created in the combustion chamber during the intake stroke tends to fall dramatically, increasing the air-fuel mixture concentration in the combustion chamber, which leads to increased volumetric efficiency. The higher the number of Revolutions Per Minute (RPM), the higher the engine traction and, consequently, the lower the pressure created inside the cylinder (Heywood, 1988). In general, manifolds should be designed to offer a minimum of resistance to flow (Garrett *et al.*, 2001).

Based on the stoichiometric ratio for the combustion of the commercial gasoline used in the vehicle, we have that, for the burning of 1 gram of commercial gasoline, it is necessary 14.7 grams of air. The introduction of restraining elements intentionally increases the pressure drop in the intake system, affecting air suction capacity, primarily by reducing the cross-sectional diameter of the intake system from 38 mm to 20 mm. The regulation of the Formula-SAE competition makes it mandatory to use flow restraint devices located between the throttle body and the engine (Fig. 1), having a maximum throttle diameter of 20.0 mm for gasoline engines (SAE, 2014).

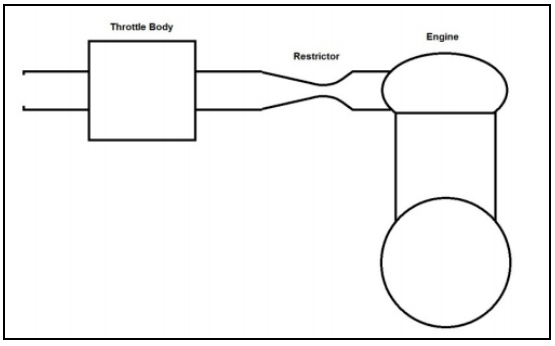

Figure 1. Location of the restrictor in the intake system.

Provase *et al.* (2014) shows that the use of flow restraint devices affects the behavior of the engine, reducing considerably the power developed by limiting the mass of air at high rotations. Hanriot *et al.* (2006) shows that by varying the engine speed of rotation a nonlinear variation of the negative pressure occurs.

The objective of this paper is to present a numerical and experimental analysis of the pressure loss generated by the insertion of the restrictor at the Scuderia Team vehicle intake manifold for the 2016 competition, measuring the impact on the admitted mass flow and the engine volumetric efficiency in varied RPM.

2. METHODOLOGY

The analysis on the vehicle intake manifold of the Scuderia Team (Fig. 2) was performed in order to measure how the insertion of a venturi-type flow restrictor between the throttle body and the intake valve inlet would affect the behavior of the vehicle. The admission system, as well as the engine to which it belongs, were transferred by the Universidade Federal da Paraíba (UFPB) to the Scuderia team of the Universidade Federal de Campina Grande (UFCG) in the year 2013 for the development of the competition vehicle.

Figure 2. Components of the vehicle's admission system for the 2016 competition. From left to right: Carburetor, restrictor and adapter for fixing to the engine head.

The engine being tested is a motor of characteristics described in Tab. 1.

Table 1. Characteristics of the Honda NX-400 engine (HONDA, 2005).

Displacement:	397.2 cm³
Number of cylinders:	Mono-cylindrical, vertical, 4-stroke DOHC
Fuel:	Gasoline (G)
Power:	Carburetor, aspirated
Piston diameter:	85 mm
Piston stroke:	70 mm
Compression ratio:	8.8:1
Max. Original Power:	30.60 CV @ 6500 RPM
Max. Original Torque:	3,51 kgf.m @ 6000 RPM
Year of manufacture:	2005

2.1 Experimental procedure

The experiment was carried out in two different situations, where the first one was given by the analysis of the original system, without insertion of the restrictor, and the second situation with the admission system carrying the restrictor.

Using the factorial analysis to identify the latent factors considered as fundamental for the experimental analysis and measurement of pressure loss, the flow bench analysis was composed of 8 trials with one repetition for each case. The variables identified as latent to the system were ambient pressure, ambient temperature and vehicle rotation speed.

The flow bench (Fig. 3) and the intake manifold (Fig. 2) were equipped with a specific set of sensors and transducers, being used to evaluate the pressure, flow rate, temperature and speed of rotation of the crankshaft.

Figure 3. Instrumentation in the engine for data acquisition.

The system developed to follow the behavior of fundamental factors in the analysis of the pressure loss and measurement of the impacts generated by the insertion of the restrictor made use of two capacitive pressure transducers Motorola MPX model with input measurement of up to 7 bar and calibrated to provide a maximum error of ± 2.5%, being allocated to the intake valve port and another employed in the region between the throttle body and the restrictor. The use of transducers in these locations is due to the need to measure the pressure loss behavior and speed at points considered strategic for the analysis. By means of a Bosch KY003 rotation sensor it was possible to analyze the pressure behavior in the main RPM ranges of the motor as well as to establish the air inlet temperatures from two Cromel type K alloys with a sensitivity of 41 μV/°C, allocated throughout the intake system.

The experimental analysis was performed at fixed intervals of 1500 RPM, starting from engine idling, set at 1500 RPM, up to 6000 RPM.

The data acquisition was performed from an electronic prototyping platform *Atmel* with assistance of programming in *Visual Studio* for treatment and storage of collected data. The experimental uncertainties of the measured parameters are in Tab. 2.

Table 2. Experimental uncertainties.

PARAMETERS	UNCERTAINTY
Pressure	101,325.00 ± 4,863.60 Pa
Temperature	± 0.48 ºC
Rotation	±50 RPM

2.2 Numerical analysis

In parallel with the experimental analysis was performed a CFD analysis of the system. Because it is an internal flow, compressible, with variation of area and presence of friction effects, heat transfer and shock waves, the equations of continuity (Eq. 1), conservation of momentum (Eq. 2), equations of the First and Second Laws of Thermodynamics (Eq. 3 and 5) and the equation of state for an ideal gas (Eq. 6) were considered. From Eq. (3), the specific energy represents the kinetic, potential and internal energy plots (Eq. 4) and, from Eq. (5), θ represents the absolute temperature and *s* the specific entropy.

$$\frac{\partial}{\partial t}\rho + \nabla.\left(\rho\vec{V}\right) = 0 \tag{1}$$

$$\frac{\partial \rho\vec{V}}{\partial t} + \nabla(\rho\vec{V}.\vec{V}) = \nabla.T + \rho\vec{g} - \rho\vec{a}_I \tag{2}$$

$$\rho\frac{De}{Dt} = \nabla(\vec{q}_k - W) \tag{3}$$

$$e = \hat{u} + \frac{1}{2}\vec{V}.\vec{V} + \vec{g}.\vec{r} \tag{4}$$

$$\frac{\partial(\rho s)}{\partial t} + \nabla.(\rho s\vec{V}) \geq \nabla.\left[\frac{k\nabla\theta}{\theta}\right] \tag{5}$$

$$p = \rho RT \tag{6}$$

The right side of Eq. (2) represents the sum of the external forces per unit volume, acting on the differential volume, in this case represented by the tensor of the fluid, *T*, due to the field of deformations of the fluid, by the gravitational field force, and also by an inertial acceleration a_I.

By the choice of permanent analysis, the time-dependent terms in the above equations were neglected as well as those dependent on gravity and, at any given speed, the depression remains constant. In practice, of course, the flow pulsates, the worst condition arising in a single cylinder four-stroke engine when the duration of the suction impulse is only approximately 25% of the total cycle time. By this choice, the occurrence of the inertial waves of depression which are reflected along the intake system when the intake valve is closed is not taken into account (Garrett *et al.*, 2001).

The CAD geometry (Fig. 4) was prepared based on the actual dimensions of the system components. The intake system is composed of a carburetor, a restrictor, with 20 degree convergence and divergence angles (Fig. 5) and an adapter for fixing to the engine head.

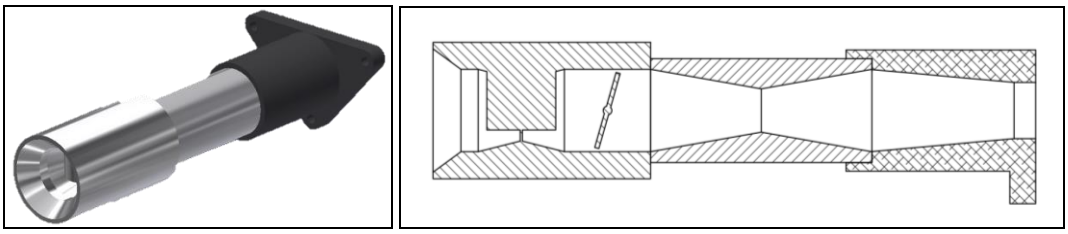

Figure 4. CAD geometry used in CFD simulations.

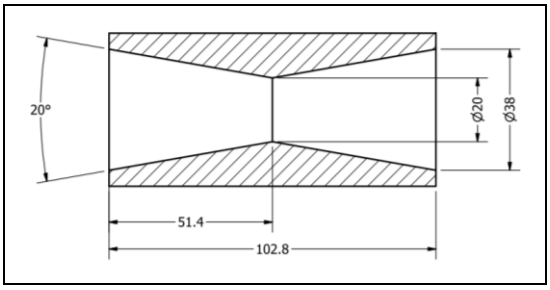

Figure 5. Detailed drawing of the geometry of the restrictor used in the vehicle for the competition of 2016. The drawing units are in millimeters.

The following boundary conditions were applied to the contour:

i. Non-slip condition on the inner walls;
ii. In the input, $u = 0$ *m/s*, $T_{amb} = 29$ *ºC* and $p_{atm} = 98{,}420$ *Pa*;
iii. At the outlet, the admitted mass flow rate measured on the flow bench (Tab. 3) was specified;
iv. The throttle valve angle and the throttle piston opening (Tab. 3) were also measured on the flow bench for each RPM;
v. On the outer wall of the restrictor, water condensation was observed due to the low temperature that the flow presents in the throat. To determine the heat transfer from the external environment to the wall of the restrictor at lower temperature, the coefficient of heat transfer by natural convection was determined to be 5.51 W/m².K.

Table 3. Geometrical parameters of the carburetor and mass flow rate for each rotation regime.

RPM	THROTTLE VALVE ANGLE	THROTTLE PISTON OPENING (mm)	MASS FLOW (kg/s)
1500	16º	5.00	$2.6\text{x}10^{-3}$
3000	35º	8.50	$2.7\text{x}10^{-3}$
4500	60º	12.00	$2.8\text{x}10^{-3}$
6000	65º	12.00	$3.0\text{x}10^{-3}$

3. RESULTS AND DISCUSSION

The results obtained by the experimental analysis demonstrated that the geometry of the restrictor being used in the vehicle for the 2016 competition is a faulty geometry, causing the vehicle to be underused.

The experimental analysis showed that at low engine speeds, when the engine requires less air, the reduction in the area is compensated by the accelerated air flow through the throat (section of 20.0 mm), generating a significant pressure loss, but not affecting volumetric efficiency. However, since the vehicle is designed to operate at medium and high speeds (3000 RPM at 6000 RPM), the throat flow reaches high speeds and the flow becomes compressible, leading to a maximum pressure difference between the atmosphere and the pressure created in the cylinder.

Table 4 quantifies the negative pressure of the experienced engine. The comparison between the original and the flow restraint systems shows a considerable drop in pressure as a function of the elevation of the rotation speed.

Table 4. Negative pressure at the outlet of the intake system as a function of the rotation regime for the system without and with the restrictor.

RPM	$P_{(ORIGINAL)}$ [Pa]	$P_{(RESTRITOR)}$ [Pa]	ΔP (ABS)	Δ (%)
1500	51,807.0196	39,791.6607	12,015.3589	23.19%
3000	53,806.3903	42,320.8352	11,485.5551	21.34%
4500	55,740.7348	45,670.3992	10,070.3356	18.07%
6000	59,287.7898	48,649.1798	10,638.6100	17.94%

For the purpose of validating the study, Tab. 5 shows the result of the pressure at the outlet of the restrictor according to a CFD analysis, showing the deviations of the experimental analysis (Tab. 4) based on this. Figure 6 shows the variation of the absolute pressure fields in the longitudinal section of the restrictor for the rates of 1500 to 6000 RPM.

Table 5. Mean pressure at the outlet of the intake system by numerical analysis and the error compared with the experimental results.

RPM	$P_{(CFD)}$ [Pa]	δ (%)
1500	39,699	-0.23%
3000	42,339	0.04%
4500	44,436	-2.70%
6000	48,778	0.26%

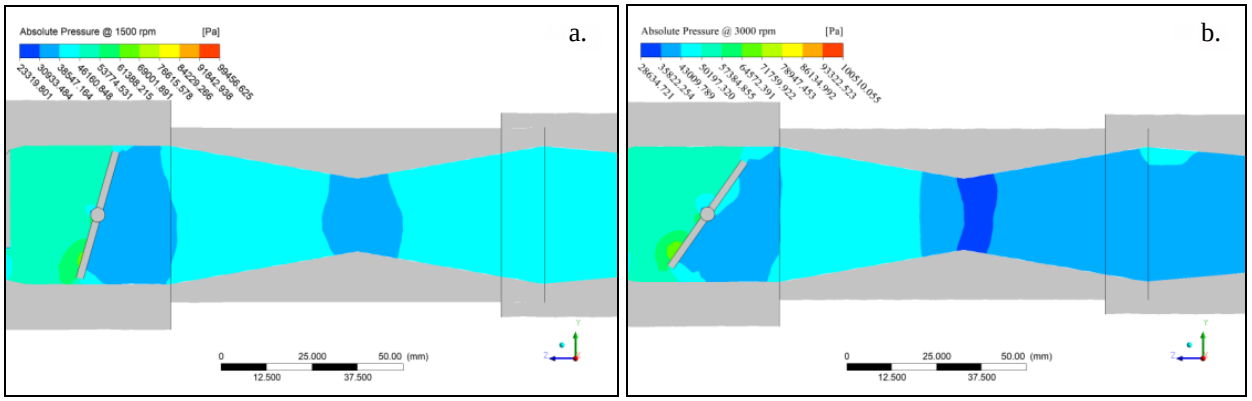

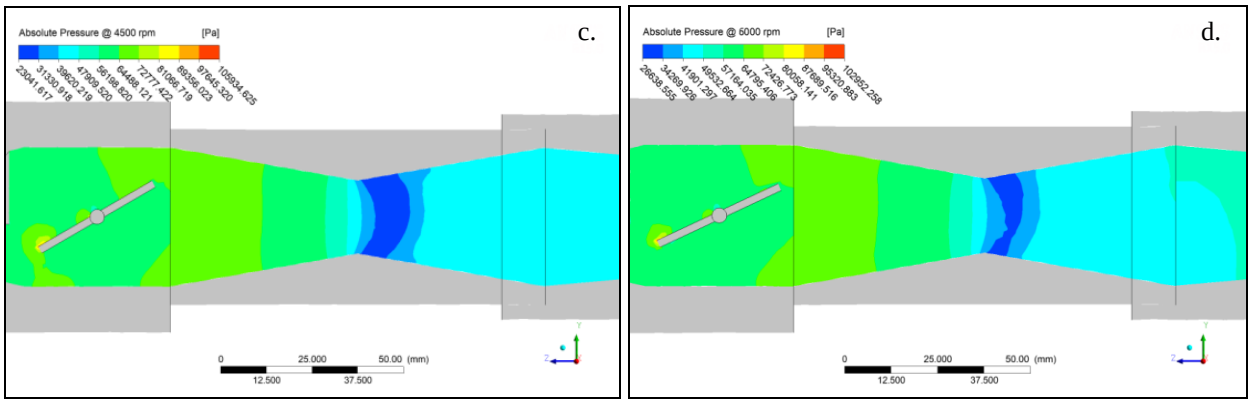

Figure 6. Distribution of the absolute pressure along the longitudinal section of the system with the restrictor for the rotation regimes of 1500 (a), 3000 (b), 4500 (c) and 6000 RPM (d).

From 3000 RPM, the appearance of a recirculation region at the exit of the restrictor was observed. From Fig. 7.a, we find that, in the diverging section, near the wall, the flow separation is formed between a high velocity flow, which is approximately sonic, and a low velocity that is practically equal to zero. The flow field is divided, in the viscous boundary layer, with the return flow and the inverse flow.

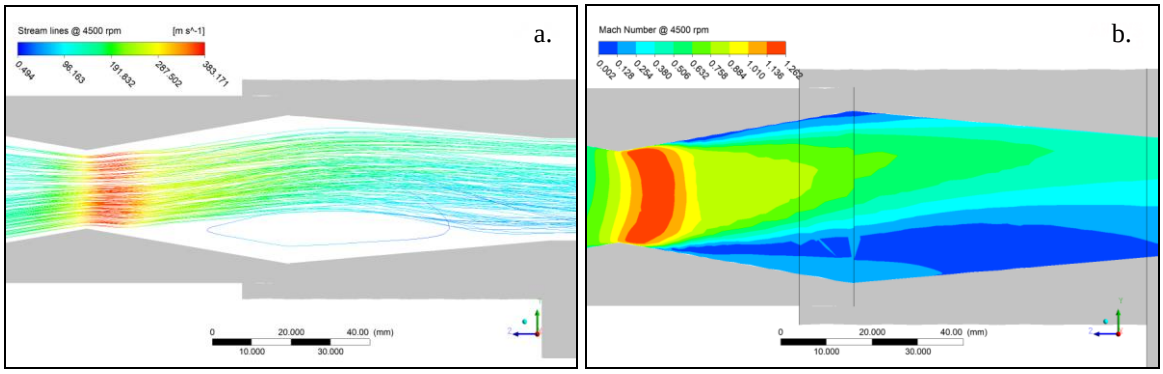

Figure 7. Three dimensional flow current lines (a) and Mach number contours (b) for 4500 RPM.

This separation region consists of oblique shock waves that merge into a growing Mach stream (Fig. 7.b). The adverse pressure gradient through the shock wave forces the boundary layer to separate, forming regions of separation downstream of the throat. The oblique shock structures result in a low supersonic flow downstream of the throat, whereas the flow immediately after the Mach current is subsonic.

The low static pressure before the edge of the shock wave leads to rapid compression and deceleration of the air flow as it enters the shocks and the high static pressure after the shocks leads to rapid expansion and acceleration.

Still in Fig. 7, there is an asymmetry of the regions of the flow separation even with a symmetric velocity field emerging from the throat. This is due to the instability of the three-dimensional flow.

The pressure loss generated at the valve port affects significantly the flow curves and the volumetric efficiency of the motor, implying significant losses. Figure 8 shows the result of the variation of the volumetric efficiency according to the rotation regime for the engine with the original intake system and with the restrictor specified by the F-SAE rules. The generated analysis shows that the admitted mass of air and the volumetric efficiency are presented as directly related to the level of pressure in the valve door that, for higher rotations, when the inlet valve is about to close, the inertia of the intake gases increases the pressure in the valve port and improves the filling of the combustion chamber and, consequently, the volumetric efficiency.

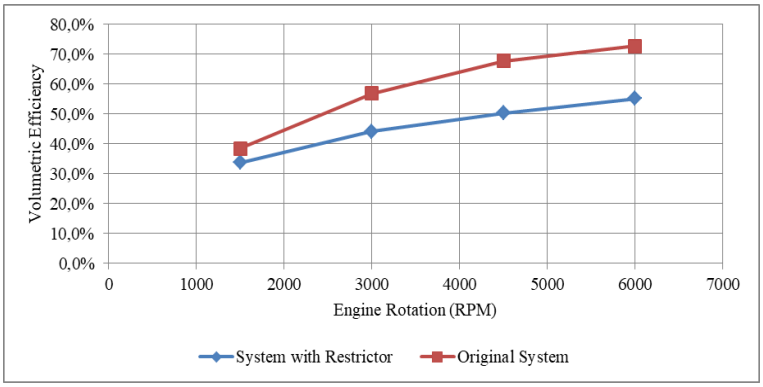

Figure 8. Comparison of the volumetric efficiencies as a function of the rotation regime.

The increase mass flow rate in the original engine is increasing throughout the range of rotations analyzed, however, when introducing the restrictor the mass flow rate tends to be reduced drastically, presenting the reduced growth rate for rotations above 4500 RPM. Figure 9 shows the results for the intake mass flow measurements from 1500 RPM to 6000 RPM regimes, indicating that they were adversely affected, generating a 25% reduction for regimes from 4500 to 6000 RPM while fuel consumption grew 17.3%.

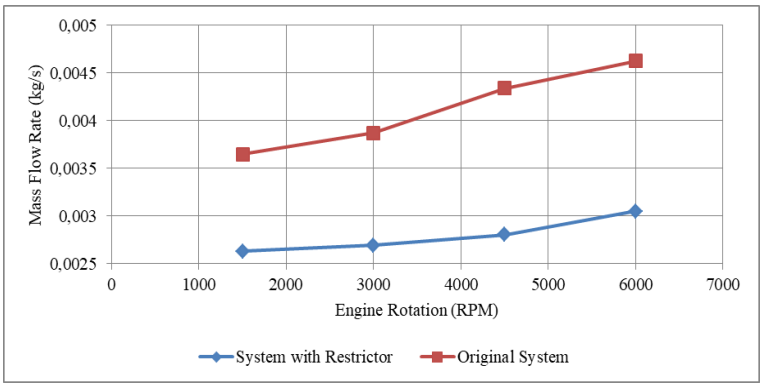

Figure 9. Comparison of the experimental mass flow rates as a function of the rotation regime.

4. CONCLUSION

Throughout the intake time, the drop generated by the reduction of pressure is a direct consequence of the introduction of the restriction device, interfering with the behavior of the pressure waves at the moment of opening of the intake valve, thus affecting the performance of the engine.

The perturbations generated by the insertion of the restrictor propagate along the alternating opening of the valves, manifesting for a finite time, which provides a process of successive compressions and expansions inside the intake manifold, forming a pressure disturbance and exciting the gases periodically.

The results were satisfactory, with a mean difference of 0.75% for the numerical and experimental analyzes. Small modifications were made to the intake system, such as polishing the inner surfaces of the restrictor, in order to increase the volumetric efficiency, however, the gain was minimum, varying from about 2.8% (3000 RPM) to a maximum of 3.1% (6000 RPM), and it is necessary to optimize the restrictor design.

5. ACKNOWLEDGEMENTS

This work was supported by the F-SAE UFCG Scudeira Team and the Department of Mechanical Engineering from UFCG and by the PET Mechanical Engineering Group (PETMEC-CG). Finally, the authors thank SESU/MEC for the financial support in the form of grants and funding for the PETMEC-CG's undergraduate researches.

6. REFERENCES

Garrett, T.K., Newton, K. and Steeds, W., 2001. *The Motor Vehicle.* Butterworth-Heinemann.

Hanriot, S.M., Huebner, R. and Coutinho, I.A. 2006. “Análise do escoamento em condutos de admissão na presença de junções”. In *Proceedings of the 11th Brazilian Congress of Thermal Engineering and Sciences – ENCIT2006*. Curitiba, Brazil.

Heywood, J.B., 1988. *Internal Combustion Engine Fundamentals*. New York: McGraw-hill,

Honda. 2005. *Manual de usuário Honda NX-400*.

Provase, I. S., Pimenta, M. de M., and Mariani, A. L. de C., 2014. “Analysis of the flow detachment in the intake manifold of a formula SAE vehicle”. 28 Mar. 2017 <http://bdpi.usp.br/single.php?_id=002713114>.

SAE, 2014. *2015-2016 Formula SAR Rules*. SAE International.

7. RESPONSIBILITY NOTICE

The authors are the only responsible for the printed material included in this paper.